Derivation of Haploid Trophoblast Stem Cells via Conversion In Vitro

Article

Derivation of Haploid Trophoblast Stem Cells via Conversion *In Vitro*

Keli Peng, Xu Li,
Congyu Wu, ...,
Yong Fan, Yang
Yu, Ling Shuai

lshuai@nankai.edu.cn

HIGHLIGHTS

A haploid cell line of
extraembryonic lineages
with self-renewal ability

haiTSCs have
multipotency to functional
trophoblast lineages both
in vitro and *in vivo*

High-throughput
screening of
spongiotrophoblast
specification-related
genes in haiTSCs

Htra1 is a blocker for
spongiotrophoblast-
specific differentiation

Article

Derivation of Haploid Trophoblast Stem Cells via Conversion *In Vitro*

Keli Peng,[1,6] Xu Li,[1,6] Congyu Wu,[2,6] Yuna Wang,[1] Jian Yu,[3] Jinxin Zhang,[1] Qian Gao,[1,5] Wenhao Zhang,[1] Qian Zhang,[1] Yong Fan,[4] Yang Yu,[5] and Ling Shuai[1,7,*]

SUMMARY

Owing to their single genome, haploid cells are powerful to uncover unknown genes by performing genetic screening in mammals. However, no haploid cell line from an extraembryonic lineage has been achieved yet, which limits the application of haploid cells in placental genetic screening. Here, we show that overexpression of Cdx2 can convert haploid embryonic stem cells to trophoblast stem cells (TSCs). p53 deletion reduces diploidization during the conversion and guarantees the generation of haploid-induced TSCs (haiTSCs). haiTSCs not only share the same molecular characterization with trophoderm-derived TSCs but also possess multipotency to placental lineages in various procedures. In addition, haiTSCs can maintain haploidy in the long term, assisted by periodic sorting and with reliance on FGF4 and heparin. Finally, we perform piggyBac-mediated high-throughput mutation in haiTSCs and use them in trophoblast lineage genetic screening. Deep sequencing analysis and validation experiments prove that Htra1 is a blocker for spongiotrophoblast specification.

INTRODUCTION

Haploid cells serve as a powerful tool in forward and reverse genetic screening owing to their single-set chromosome feature (Shuai and Zhou, 2014). To date, haploid embryonic stem cells (haESCs) have been achieved in many species assisted by Hoechst 33342 staining and fluorescence-activated cell sorting (FACS) (Leeb and Wutz, 2011; Sagi et al., 2016), which are important for recessive gene discovery (Elling et al., 2011; Leeb et al., 2014). Recent derivation of haploid somatic cell lines has facilitated lineage-specific genetic screening (He et al., 2017; Gao et al., 2018). Nevertheless, all haploid cell cultures prefer to double back to diploids, the mechanism of which is still unclear. According to previous reports, the addition of cell cycle inhibitors (Takahashi et al., 2014; He et al., 2017) or editing of specific genes (Olbrich et al., 2017; He et al., 2018) can stabilize the haploid genome and reduce self-diploidization to some degree. However, no haploid cell line has been reported for an extraembryonic lineage. Trophoblast stem cells (TSCs) are one type of placental progenitor cell and are derived from blastocysts or the extraembryonic ectoderm of implantation embryos (Tanaka et al., 1998). They can self-renew by relying on FGF4 and heparin (F4H *in vitro* and retain the potential to contribute exclusively to the placenta (Oda et al., 2006). Therefore the derivation of TSCs provides considerable insight into the mechanisms that regulate extraembryonic lineage specification and placental development.

Previously, haploid cells were shown to be detectable in preimplantation blastocysts (Liu et al., 2002) and implantation epiblast-stage embryos (Shuai et al., 2015), which indicated that haploid cells were reasonable in trophectoderm (TE) lineages. By regulating the expression of *Oct4* and *Cdx2*, embryonic stem cells (ESCs) and TSCs could switch from one to the other easily (Niwa et al., 2005; Wu et al., 2011). In addition, transcriptional induction reprograms somatic cells to functional TSCs (Kubaczka et al., 2015; Benchetrit et al., 2015), suggesting that overexpression of TSC-specific transcription factors can commit cell fate to TE lineages. Hence, haESCs may have the potential to be converted to haploid-induced TSCs (haiTSCs) via overexpression of *Cdx2*.

Here, we overexpressed *Cdx2* in haESCs by using a Tet-On inducible system to alternate cell fate. We demonstrated that haiTSCs were generated from *p53*-deleted haESCs *in vitro* under defined conditions. haiTSCs maintained haploidy and contributed to the placenta in a chimeric experiment, proving that they potentially differentiated into functional trophoblast terminal cells. Then we performed a proof-of-concept screening in haiTSCs to identify key genes regulating spongiotrophoblast specification.
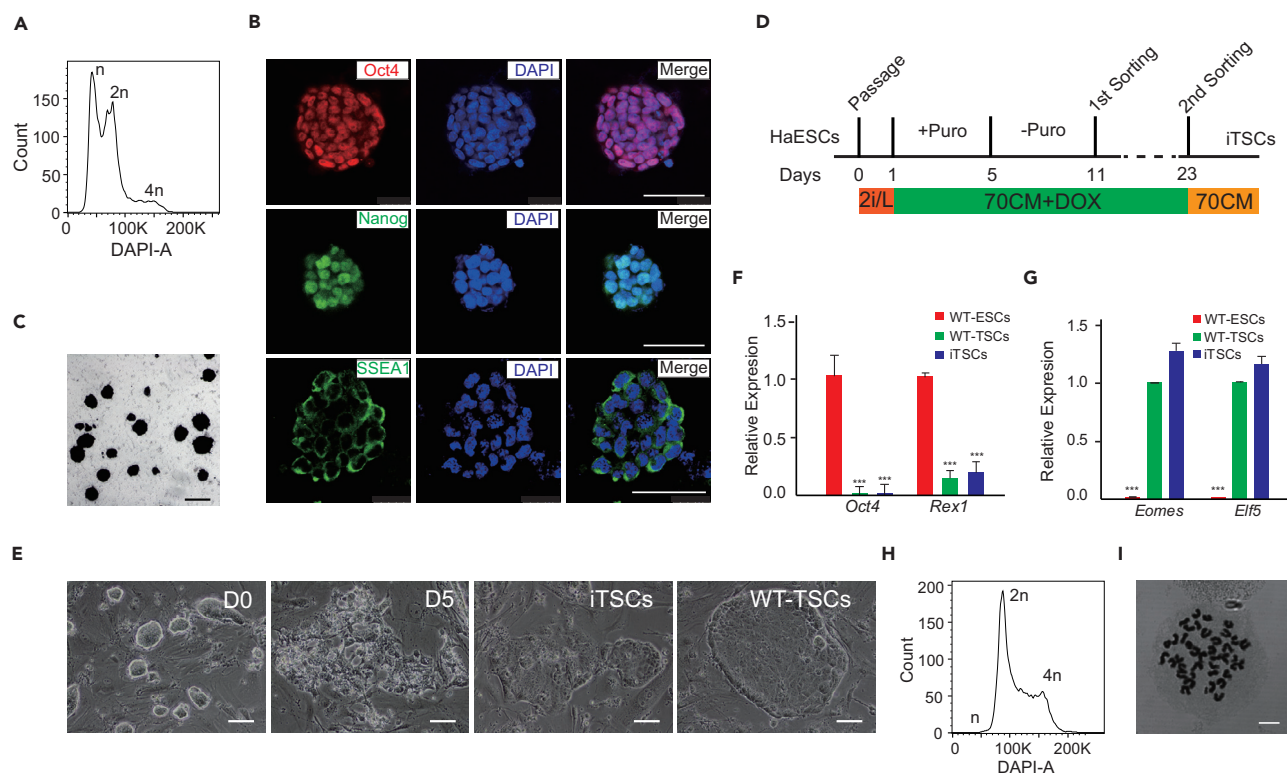
Figure 1. Overexpression of *Cdx2* Converts haESCs to TSCs

(A) DNA content analysis of haESCs. The percentage of 1n (G0/G1) peak was 50.2%.

(B) Immunofluorescence staining of pluripotent markers (Oct4, Tetramethylrhodamine [TRITC] channel; Nanog and SSEA1, fluorescein isothiocyanate channel) in haESCs. DNA is stained with DAPI. Scale bar, 50 μm.

(C) Alkaline phosphatase-stained haESCs cultured on mouse embryonic fibroblasts. Scale bar, 100 μm.

(D) Schematic overview of iTSC derivation from haESCs via *Cdx2* overexpression.

(E) The morphological changes of colonies during the conversion process. WT-TSCs are used as control. Scale bar, 100 μm.

(F) The expression levels of pluripotent marker genes (*Oct4* and *Rex1*) in iTSCs, WT-TSCs, and WT-ESCs by qPCR. t test, ***p < 0.001. Data are represented as mean ± SEM.

(G) The expression levels of TSC marker genes (*Eomes* and *Elf5*) in iTSCs, WT-TSCs and WT-ESCs. t test, ***p < 0.001. Data are represented as mean ± SEM.

(H) DNA content analysis of iTSCs derived from haESCs. The results indicated that there were no haploid cells in the iTSCs.

(I) Chromosome spreads of iTSCs. Each single cell spread had 40 chromosomes. Scale bar, 7.5 μm.

See also Figures S1 and S2.

RESULTS

Overexpression of *Cdx2* Converts haESCs to TSCs

To generate haiTSCs from haESCs by conversion *in vitro*, we adopted an inducible overexpression strategy. Parthenogenetic haESC lines were established from 129Sv/Jae background chemical-activated oocytes, and one line with a high percentage of haploid cells was chosen to perform subsequent experiments (Figure 1A). We then designed two *piggyBac* (PB) vectors to introduce Tet-On inducible *Cdx2* overexpression into haESCs: vector 1 had the rtTA (Tet-On Advanced transactivator) and *neomycin* selection genes, driven separately by an SV40 promoter, and vector 2 had the *Cdx2* and *puromycin* resistance genes, driven by a tetracycline response element with a minimal cytomegalovirus promoter (Figure S1A). We transfected these two PB vectors and a PBase vector into haESCs by electroporation. Transfected cells were selected in 2i/L (inhibitor PD0325901, inhibitor CHIR99021, and mLif) medium (Ying et al., 2008), supplemented with G418 (250 μg/mL) for 6 days. To evaluate the pluripotency of the transfected haESCs (which we termed OE-Cdx2 haESCs), we performed immunofluorescent staining of pluripotent markers and alkaline phosphatase (AP) staining. The results showed that OE-Cdx2 haESCs were positive not only for Oct4, Nanog, and SSEA1 (Figure 1B) but also for AP (Figure 1C), which demonstrated that vector insertion did not jeopardize haESC pluripotency. Thereafter we cultured newly sorted haploid OE-Cdx2

haESCs in standard TSC culture medium supplemented with doxycycline (Dox) and puromycin to induce *Cdx2* overexpression (Figure 1D). Obvious morphological change was observed 5 days after Dox induction, and many cells died during puromycin selection. Approximately 11 days after induction, typical TSC-like colonies were formed (Figure 1E) and expanded with trypsin, which meant that an inducible TSC (iTSC) line was established. Immunofluorescence results revealed that iTSCs expressed the TSC-specific markers Cdx2 and Eomes, rather than the ESC marker Oct4 (Figure S2D). Quantitative PCR (qPCR) results further confirmed that iTSCs did not express pluripotent genes (*Oct4* and *Rex1*) relative to wild-type (WT) ESCs (Figure 1F) and showed similar expression levels of TSC markers (*Eomes* and *Elf5*) relative to WT-TSCs (Figure 1G). Therefore iTSCs were derived by conversion of haESCs *in vitro* through *Cdx2* overexpression.

We utilized Hoechst 33342 staining and FACS to isolate haploid cells during conversion. After optimization, we first sorted the haploid cells on day 11 post conversion; the 1n peak (haploid cells) was 4.38% and was further expanded with good viability (Figure S1B). There was no haploid cell left among the iTSCs according to the second round of sorting by FACS (Figures 1H and S2C) and chromosome spread analysis (Figure 1I). We reasoned that different PB insertions might affect haploid maintenance ability; thus we randomly picked six subclones from among OE-Cdx2 haESCs. We genotyped the subclones, and the results suggested that all subclones carried *Cdx2* and rtTA (Figure S1C). Among the six subclones, #1 and #2 were stable in terms of haploid maintenance and were further assessed (Figure S2A). Although #1 and #2 carried a few insertions (Figure S1D) and could be converted to typical iTSCs easily (Figure S2B), neither of them could generate haiTSC lines (Figure S2C). We reasoned that the nature of diploidization in haESCs during conversion hindered the derivation of haiTSCs.

Deletion of *p53* Facilitates Derivation of HaiTSCs

A previous study showed that *p53* gene deficiency could stabilize haploidy in mouse haESCs by promoting the viability and proliferation of haploid cells in daily culture (Olbrich et al., 2017). To achieve haiTSCs in our OE-Cdx2 system, we knocked out *p53* in OE-Cdx2 haESCs through CRISPR/Cas9-mediated non-homologous end joining. We transfected plasmids carrying Cas9-GFP and two single guide RNAs (sgRNAs, targeting the third exon of *p53*) (Figure S3B) into OE-Cdx2 haESCsubclone #1, which had a high percentage of haploid cells (Figure 2A). Approximately 36 hr after transfection, haploid cells expressing Cas9-GFP were enriched by FACS (Figure S3A). To address whether *p53* deletion occurred, we randomly picked four subclones (we termed them PO1, PO2, PO3, and PO4) and performed T7 endonuclease I (T7ENI) cleavage analysis. The results showed that all subclones underwent gene editing (Figure S3C). Further sequencing results confirmed that all four subclones carried mutations with small deletions at the target sites (Figure S3D). We also detected p53 at the protein level in PO1 and PO4 by western blot and found that the p53 protein was absent in these subclones (Figure 2B). Furthermore, we analyzed the expression levels of *p53*-related genes in PO1 and PO4 by qPCR relative to a WT-ESC line. *p53* and *P21* in PO1 and PO4 were downregulated, whereas other cell cycle genes, including *Reprimo*, *Cdk1*, and *Cyclin B*, exhibited no significant differences (Figure 2C). Taken together, the results indicated that *p53* deletion was successfully realized in OE-Cdx2 haESCs.

To determine whether *p53* mutation could stabilize haploidy in OE-Cdx2 haESCs, we used a serum ESC medium without 2i (Elling et al., 2011) to trigger severe diploidization. We cultured PO1, PO2, PO3, and PO4 separately in this serum ESC medium for five passages without sorting and found that the PO4 cell line maintained haploidy at a very high percentage relative to the other subclones (Figure S3E). In another repeat trial, we cultured PO4 and #1 in 2i/L medium; 40.2% of PO4 cells remained in the 1n peak (haESCs at G0/G1 phase), whereas the 1n peak percentage in #1 was reduced to 16% during the same period (Figure S3F). Given that PO4 with *p53* deletion maintained haploidy in a steady manner, we performed conversion with PO4 to derive haiTSCs with Dox and puromycin monitoring. After conversion for approximately 11 days and three subsequent rounds of haploidy purification by FACS (Figure S3G), a haploid cell line was established and showed mostly one set of chromosomes by FACS (Figure 2D) and karyotype analysis (Figure 2E). To enrich authentic haiTSCs from these haploid derivatives, we purified them with the TSC-specific antibody CDCP1 (Rugg-Gunn et al., 2012). The FACS results showed that approximately 39.7% of cells were already CDCP1 positive (Figure 2F); these cells were harvested and further cultured in either feeder or feeder-free culture systems with typical TSC colony morphology (Figure 2G). Immunofluorescence staining results revealed
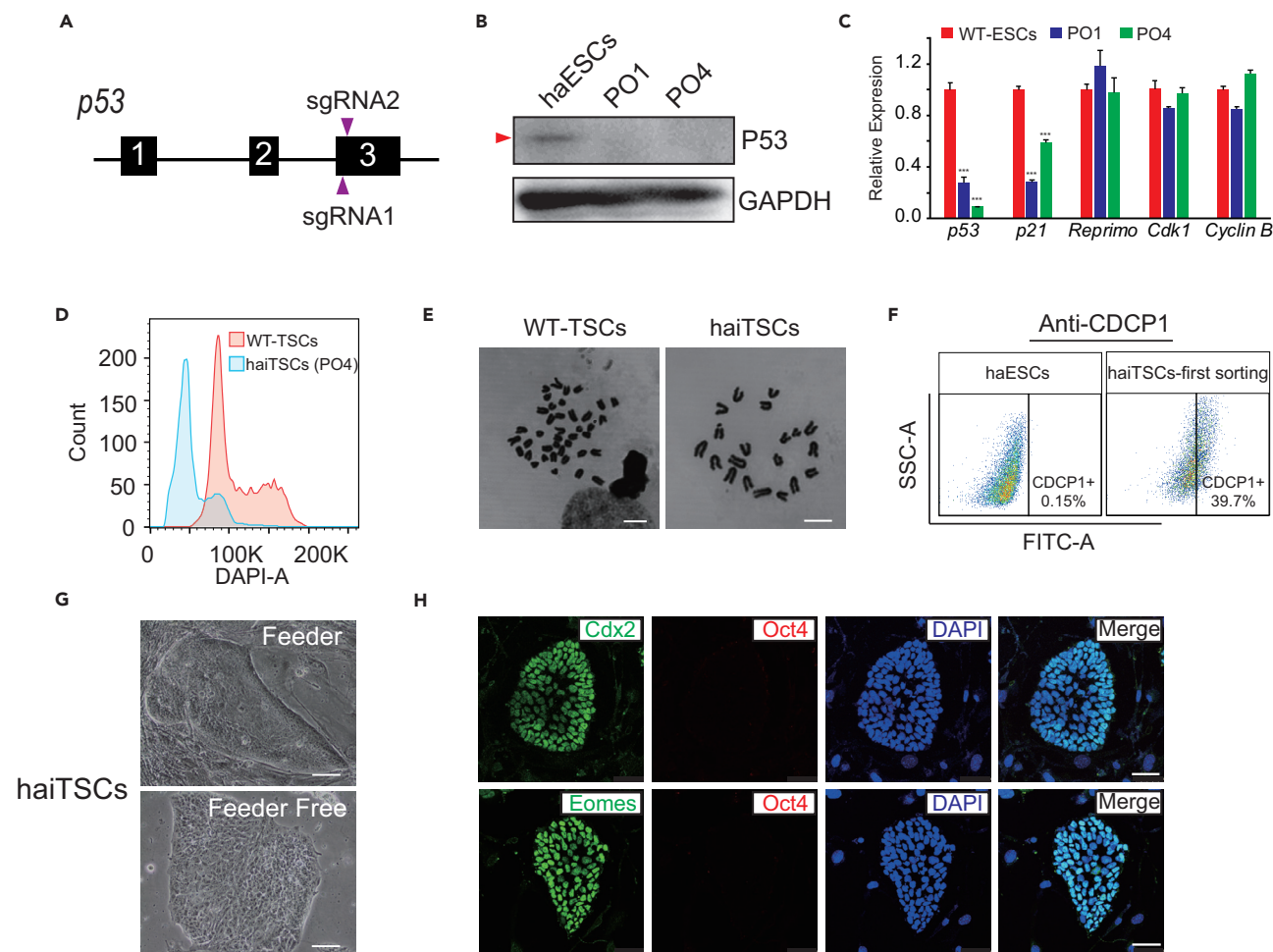
Figure 2. Deletion of p53 Facilitates Derivation of haiTSCs

(A) Schematic diagram of the strategy to knock out p53 via the CRISPR/Cas9 system. The two sgRNAs are designed to target exon 3 of p53.

(B) Western blot to detect p53 in PO1, PO4, and WT-haESCs. GAPDH is used as a loading control.

(C) The expression levels of p53-related genes and cell-cycle-related genes (*p53*, *P21*, *Reprimo*, *Cdk1*, and *CyclinB*) in PO1, PO4, and WT-ESCs by qPCR. t test, ***$p < 0.001$. Data are represented as mean $\pm$ SEM.

(D) DNA content analysis of haiTSCs derived from the cell line PO4. The percentage of the 1n (G0/G1) peak was 70.4%. Diploid WT-TSCs are used as a control.

(E) Chromosome spreads of haiTSCs and WT-TSCs. haiTSCs have a 20-chromosome set, whereas WT-TSCs show 40 chromosomes in a single cell. Scale bar, 7.5 μm.

(F) TSC-specific CDCP1 antibody analysis of derived haiTSCs at first sorting. The percentage of CDCP1-positive cells is 39.7%.

(G) Images of haiTSCs colonies on feeder cells and on Matrigel. Scale bar, 100 μm.

(H) Immunofluorescence staining of TSC markers (Cdx2 and Eomes, fluorescein isothiocyanate channel) and pluripotent markers (Oct4, Tetramethylrhodamine [TRITC] channel) in haiTSCs. DNA is stained with DAPI. Scale bar, 50 μm.

See also Figure S3.

that haiTSCs expressed the TSC-specific markers Cdx2 and Eomes instead of the ESC marker Oct4 (Figure 2H).

Molecular Characterization and Differentiation Potentials of haiTSCs

To assess the purity of haiTSCs after CDCP1-positive cell sorting, we passaged them several times and reanalyzed them with the CDCP1 antibody by FACS. CDCP1-positive cells remained at a high percentage (92.3%) in haiTSCs, which meant that haiTSCs could sustain TE identity during self-renewal (Figure 3A). The CDCP1-antibody-purified haiTSCs were expanded several times (three passages), and 15.3% of
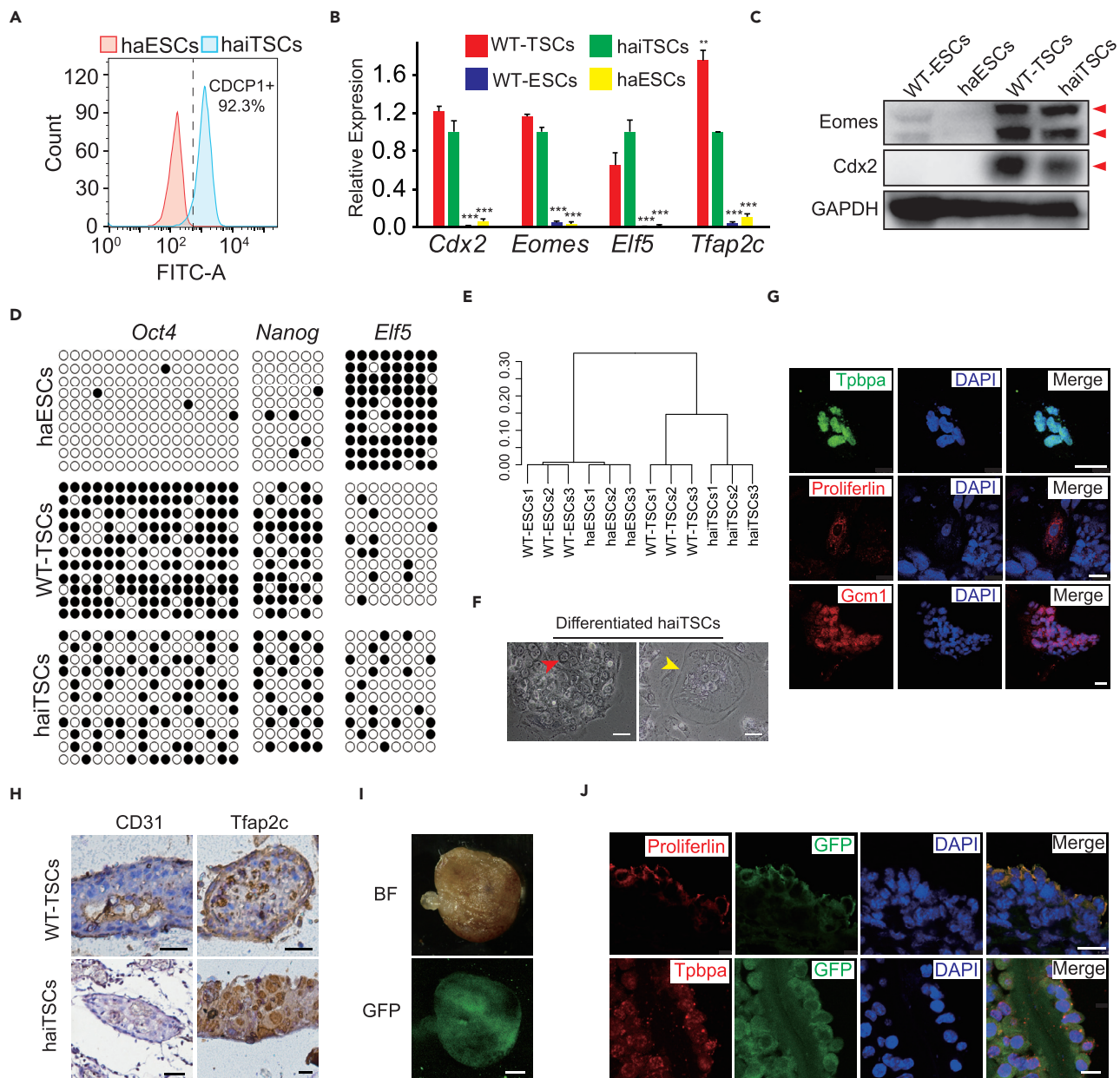
Figure 3. Identification of haiTSCs Properties and Differentiation Potential

(A) FACS analysis of CDCP1-positive cells among established haiTSCs. haESCs are used as negative control.

(B) The expression levels of TSC-specific marker genes (*Cdx2*, *Eomes*, *Elf5*, and *Tfap2c*) in haiTSCs, WT-TSCs, haESCs, and WT-ESCs. t test, **p < 0.01, ***p < 0.001. Data are represented as mean ± SEM.

(C) Western blot analysis of Eomes and Cdx2 in WT-ESCs, haESCs, WT-TSCs, and haiTSCs. GAPDH is used as a loading control.

(D) DNA methylation status in the promoter regions of *Oct4*, *Nanog*, and *Elf5*. An haESCs line and a WT-TSCs line were used as controls.

(E) Global gene expression cluster analysis of transcripts in WT-ESCs, haESCs, WT-TSCs, and haiTSCs.

(F) Images of differentiated haiTSCs. Red arrow indicates syncytiotrophoblast cells, and yellow arrow indicates trophoblast giant cells. Scale bar, 100 μm.

(G) Immunofluorescence staining of three trophoblast-lineage-specific markers, Tpbpa (fluorescein isothiocyanate channel), proliferin (Tetramethylrhodamine [TRITC] channel), and GCM1 (TRITC channel), in cells differentiated from haiTSCs *in vitro*. DNA is stained with DAPI. Scale bar, 25 μm.

(H) Immunohistochemical (IHC) analysis of hemorrhagic lesions derived from haiTSCs. Fixed sample is IHC stained against the endothelial marker CD31 and the trophoblast marker Tfap2c.

(I) Images of BF (top) and GFP (bottom) of a chimeric placenta following blastocyst injection of haiTSCs-eGFP cells. Scale bar, 2 mm.

(J) Immunofluorescence staining of chimeric placenta following sectioning, with trophoblast-lineage-specific antibodies against proliferin and Tpbpa. Scale bar, 25 μm.

See also Figures S4 and S5.

haploid cells remained (Figure S4A), indicating that haiTSCs could maintain haploidy in a TSC-specific manner. qPCR further confirmed that the expression levels of TSC-specific genes (*Cdx2*, *Eomes*, *Elf5*, and *Tfap2c*) were high in haiTSCs and WT-TSCs (Figure 3B), whereas expression levels of pluripotent genes (*Oct4* and *Nanog*) in haiTSCs and WT-TSCs were much lower than those in haESCs and WT-ESCs (Figure S4B). Western blot results also suggested that haiTSCs and WT-TSCs were positive for Cdx2 and Eomes relative to ESCs (Figure 3C). DNA-methylation-mediated gene regulation is crucial in the determination of specific transcription factors, which are extensively utilized to judge cell identities (Wu et al., 2011). We analyzed the DNA methylation status of the *Oct4*, *Nanog,* and *Elf5* promoters in haiTSCs by performing bisulfite sequencing, with haESCs and WT-TSCs as controls. Results revealed that the *Elf5* promoter in haiTSCs was hypomethylated, whereas the *Oct4* and *Nanog* promoters in haiTSCs were hypermethylated (Figure 3D), which were consequent with previous report (Ng et al., 2008). To elucidate the properties of haiTSCs on the transcriptome scale, we analyzed the global RNA levels of haiTSCs by performing RNA sequencing (RNA-seq). Cluster analysis revealed that haiTSCs resembled WT-TSCs but were distinct from either haESCs or WT-ESCs (Figures 3E and S4C). As female WT-TSCs exhibit an inactive X chromosome in a single cell, we assessed the state of the sole X chromosome in haiTSCs by costaining for histone 3 lysine 27 trimethylation (H3K27me3) and Cdx2, with female and male WT-TSCs as controls. Only H3K27me3 in female WT-TSCs (XX) accumulated in the nuclei, visualized as bright spots; however, H3K27me3 in both haiTSCs and male WT-TSCs (XY) was located all over the nuclei (Figure S4D), which indicated that the X chromosome in haiTSCs was active.

To test the differentiation potential of haiTSCs, we cultured the haiTSCs by withdrawing FGF4, heparin, and mouse embryonic fibroblasts *in vitro*. Obvious polyploidy trophoblast giant cells (TGCs) and syncytiotrophoblast (SyT) cells were observed (Figure 3F) and increased gradually (Figure S5A). Immunofluorescence staining also revealed that the spongiotrophoblast-cell-specific marker Tpbpa, the TGC-specific marker proliferin, and the labyrinth-progenitor-specific marker Gcm1 were observed in differentiated cells from haiTSCs (Figure 3G). We analyzed trophoblast-lineage-specific gene expression levels of differentiated cells (4 days) from haiTSCs, iTSCs (diploid), and WT-TSCs by qPCR. Accordingly, differentiated cells from haiTSCs expressed all lineage-specific genes; in particular, *Ctsq*, *Prl2d1*, and *Tpbpa* increased significantly (Figure S5B). Taken together, the results indicated that haiTSCs could differentiate into diverse trophoblast lineage cells *in vitro* by random differentiation. To investigate the *in vivo* differentiation potential of haiTSCs, we transplanted approximately 1×10^6 haiTSCs into the testis of ICR mice, with WT-TSCs and ESCs as parallel controls. After 3 weeks, hemorrhagic lesions formed in the haiTSC and WT-TSC groups, whereas teratomas formed in the ESC group (Figure S5C). Blood vessels with TGC invasion were confirmed in haiTSC-derived hemorrhagic lesions by immunohistochemical staining of Tfap2c and CD31 (Figure 3H), indicating that haiTSCs could mimic placental development by undergoing differentiation *in vivo*. Next, we microinjected GFP-labeled haiTSCs into blastocysts to test whether they could contribute to functional placenta. In the reconstructed blastocysts, the GFP-positive haiTSCs integrated into the TE instead of the inner cell mass (ICM), showing their trophoderm nature (Figure S5D). To evaluate further development, the reconstructed embryos were transferred to the uteruses of pseudopregnant mice. On embryonic day 10.5 (E10.5), placentas and embryos were dissected from the pseudopregnant mice. We found GFP-positive cells contributing to the placentas (Figure 3I), and these cells were positive for proliferin and Tpbpa antibody staining according to fluorescence histology analysis (Figure 3J). Our findings revealed that haiTSCs could not only mimic placental development *in vivo* but also contributed to functional placenta, which are typical features of trophoblast progenitor cells.

piggyBac Transposon-Mediated High-Throughput Gene Trapping in haiTSCs

Haploid cells are easy to use for generating genome-wide homozygous mutant libraries via PB integration or virus infection (Li and Shuai, 2017). To determine the feasibility of using haiTSCs in this process, approximately 1×10^7 haiTSCs were transfected with PB-based gene trap vectors (Leeb and Wutz, 2011) carrying a *puromycin* resistance (Puro^r) gene (Figure 4A). After 4 days of puromycin selection, integrated haiTSCs with the Puro^r gene survived, and the control group mostly died (Figure 4B). We analyzed the mutant haiTSCs by FACS and found that 38.1% of haploid cells remained, suggesting high efficiency for obtaining homozygous mutant haiTSCs (Figure 4C). We harvested mutant haiTSCs and amplified the integration sites by performing splinkerette PCR. Obvious strands demonstrating integration were visualized (Figure 4D). We linked the products into plasmids and sequenced them by Sanger sequencing. In total, 50 different sites were addressed, of which 24 were located inside the gene body (Figures S6A
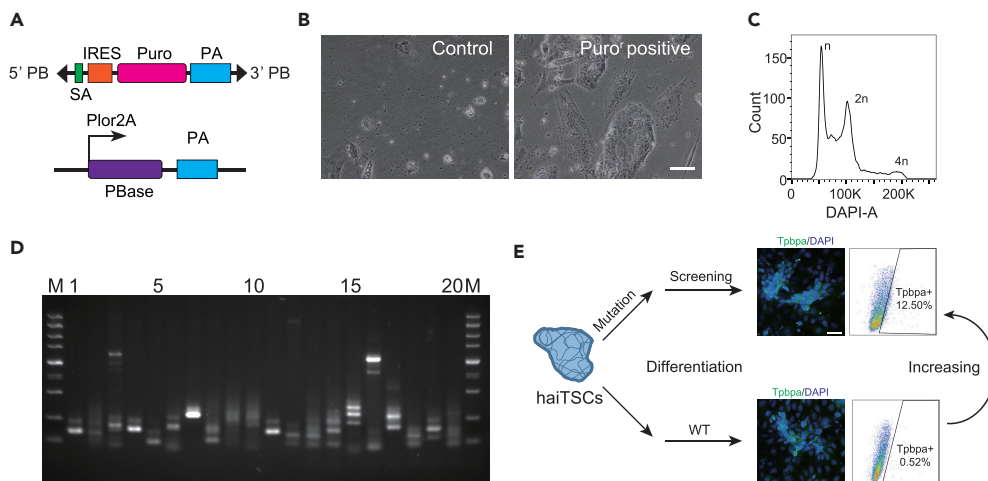
Figure 4. High-throughput Mutaion and Genetic screening in Derived haiTSCs

(A) Schematic diagram of *piggyBac*-based gene trapping vectors. The PB vector contains: 5′ PB and 3′ PB, the inverted terminal repeats (ITRs); SA, splice acceptor; IRES, internal ribozyme entry site; Puro, the coding region of puromycin resistance gene; and PA, the poly(A) sequence; the PBase vector includes Plor2A, the promoter of pbase; the Pbase, the coding sequence region of Pbase; and PA.

(B) haiTSCs transfected with *piggyBac*-based gene trapping vectors are selected by puromycin for 4 days. haiTSCs without transfection are used as a control. Scale bar, 100 μm. After selection, only transfected haiTSCs can survive.

(C) DNA content analysis of haiTSCs after transfection and puromycin selection. The percentage of the 1n (G0/G1) peak was 38.1%.

(D) Splinkerette PCR analysis of the transposition sites in the mutant haiTSCs. Each lane corresponds to one subclone; each strand corresponds to one PB integration.

(E) Schematic diagram of screening for relevant genes in Tpbpa-positive cell. Random differentiation was performed with mutated and nonmutated haiTSCs cells independently for 3 days. Immunofluorescence staining (Tpbpa, left panel), FACS analysis, and sorting of Tpbpa-positive cells (right panel).

See also Figure S6.

and S6B). These data indicate that haiTSCs could undergo gene manipulation and generate homozygous mutant libraries.

To apply haiTSCs in trophoblast lineage-specific genetic screening, we focused on key genes regulating spongiotrophoblast differentiation and utilized a specific antibody against Tpbpa (Latos and Hemberger, 2016) as indicated. Briefly, we performed random differentiation in mutated haiTSCs, as previously described, and nonmutated haiTSCs separately for 3 days. Tpbpa-positive cells demonstrating spongio-trophoblast features were analyzed by immunostaining and FACS (Figure 4E). If the percentage of Tpbpa-positive cells increased significantly in the mutated haiTSCs group relative to the nonmutated haiTSCs group, the mutated Tpbpa-positive cells were harvested with a FACS-assisted antibody for further bioinformatics analysis. We performed this experiment several times and deep-sequenced two repeats with the Tpbpa-positive cells increasing group (Figures 4E, S6C, and S6D). According to deep sequencing, approximately 4 million independent insertions across more than 20,000 genes were identified, of which 49.8% were derived from the sense orientation (Figure 5A). In addition, approximately 57% of the insertions were located in intragenetic regions (coding regions + intron + 5′/3′ UTR), whereas 39% of insertions landed in intergenetic regions (Figure 5B). Enrichment analysis with gene ontology databases showed that insertions preferred genes carrying specific functions for epigenetic modifications, such as repressing transcription factor binding and DNA methyltransferase activity (Figure 5C). Ten genes, including *Zfp704*, *Htra1*, and *Rsf1*, were identified (Figure 5D) due to both frequent insertions determined by PB screening and higher transcription activity measured from RNA-seq (Figures 5E and S7). Of the top candidates, *Htra1* was chosen for further validation experiments in WT-TSCs (Figure 5E).

Htra1 As a Blocker for Spongiotrophoblast Differentiation

To testify whether *Htra1* is an essential block against spongiotrophoblast differentiation in TSCs, we designed specific sgRNAs to knock out *Htra1* in WT-TSCs with the CRISPR/Cas9 system (Figure 6A). We
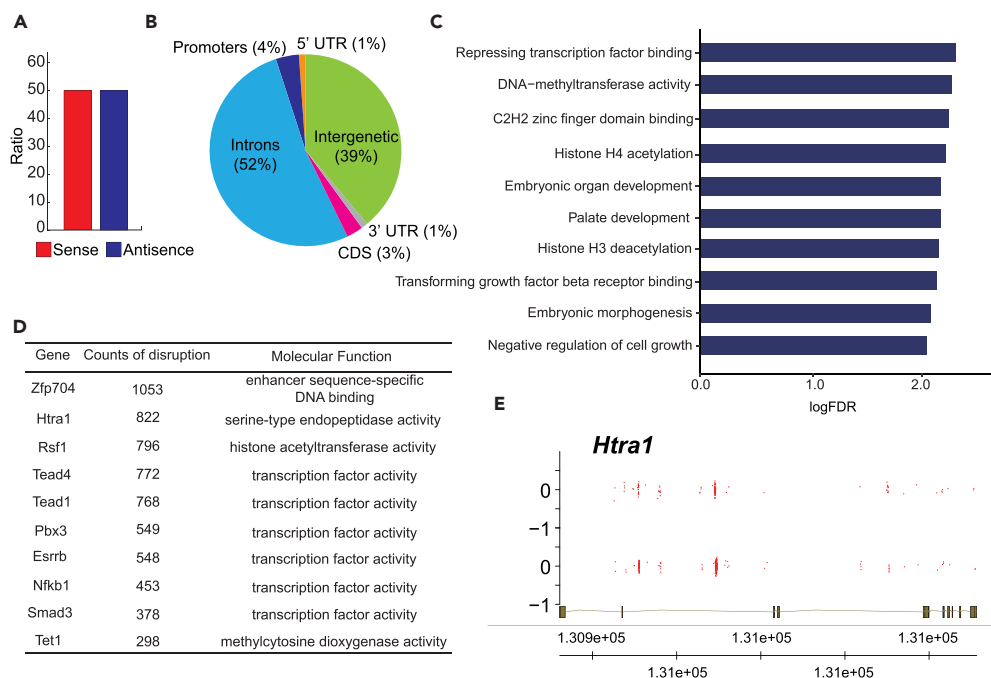
Figure 5. Bioinformatics Analysis of Integrations in haiTSCs

(A) Proportion of insertional orientation (sense/antisense) after *piggyBac* integration. A total of 49.8% insertions were derived from the sense orientation.

(B) Proportion of integration sites across various genomic regions: promoters (1 kb upstream of the transcription starting sites), 5′ UTR, exons, introns, 3′ UTR, and intergenic regions. Genome-wide PB transposon integration site analysis. Promoter region is identified as the 5-kb region upstream of a known gene.

(C) Enriched gene ontologies of the top 100 genes with the most frequent insertions.

(D) List of the top 10 genes with the most insertion sites.

(E) Strand-specific coverage tracks of the gene Htra1 for the selected library (red). Gene model and chromosome coordinates are shown at the bottom.

See also Figure S7.

transfected TSCs with a Cas9-sgRNAs vector (targeted), and control TSCs were transfected with an empty vector (mock). We performed random differentiation independently with the targeted TSCs (gene edited) and mock TSCs (non-gene edited) for 3 days. Spongiotrophoblast cells were observed by morphology (Figure 6B) analysis and Tpbpa antibody immunostaining (Figure 6C). According to a FACS analysis, the percentage of Tpbpa-positive cells in the targeted group significantly increased relative to the mock TSCs group (Figure 6D). In a parallel experiment, we analyzed the expression levels of trophoblast-lineage-specific markers in differentiated cells from the targeted and mock groups and found that the expression level of the spongiotrophoblast-specific marker Tpbpa in the targeted group increased significantly relative to the mock group, whereas the other two lineage markers in the targeted group decreased (Figure 6E). We tested the genotypes of targeted TSCs, and the results indicated that the cells carried a gene mutation in *Htra1* (Figure 6F). Thus *Htra1* plays a very important role in spongiotrophoblast specification.

DISCUSSION

In this study, we demonstrate that haiTSCs can be generated by the conversion of haESCs *in vitro* and maintain haploidy well, with the potential to differentiate into placental cells. We utilized a Dox-inducible Tet-On system to introduce *Cdx2* overexpression in haESCs, which was reported to be a key regulator of TE development (Strumpf et al., 2005). Although a severe diploidization phenomenon was observed during ESC-TSC conversion, we adopted two strategies to establish haiTSCs: (1) knock out *p53* in the initial OE-Cdx2 haESCs to stabilize the haploid genome and (2) modify the TSC-specific culture system to promote cell fate alternation (including specific growth factors and inhibitors, TSC-specific antibody sorting, etc.). With these modifications, our haiTSCs maintained haploidy stably through *p53* gene
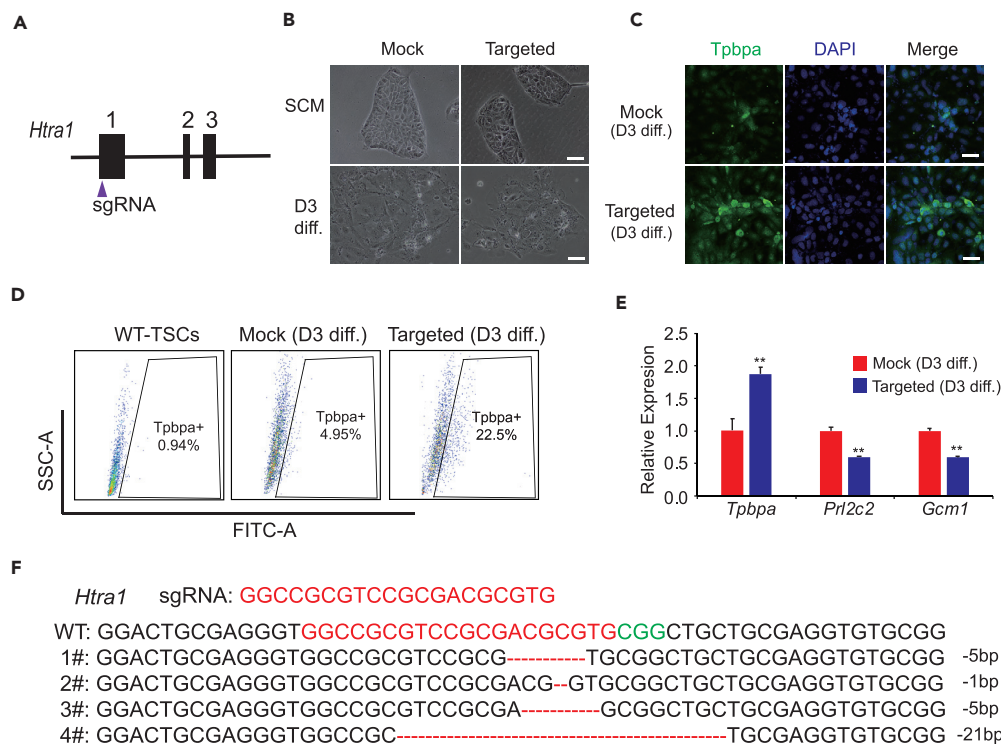
Figure 6. Validation of Candidate Genes in a WT-TSC Differentiation Assay

(A) Schematic diagram of the strategy to knock out *Htra1* in WT-TSCs using the CRISPR/Cas9 system.

(B) Bright-field images of TSCs and differentiated cells from the non-gene-edited group (mock) and the gene edited group (targeted). Scale bar, 100 μm.

(C) Immunofluorescence staining for Tpbpa (fluorescein isothiocyanate channel) in differentiated cells of the mock group and targeted group. DNA is stained with DAPI. Scale bar, 50 μm.

(D) FACS analysis of Tpbpa-positive cells in WT-TSCs, the mock group (differentiation for 3 days), and the targeted group (differentiation for 3 days). The percentage of the targeted group is 22.5%, which is higher than that of the mock group (4.95%).

(E) The expression levels of trophoblast-lineage-specific genes (*Tpbpa*, *Prl2c2,* and *Gcm1*) in differentiated cells (day 3) from the mock group and targeted group. t test, **p < 0.01. Data are represented as mean ± SEM.

(F) *Htra1*-deleted genotypes in the targeted group.

deletion and guaranteed their potential in a subsequent gene trapping procedure. The results proved that the *p53* gene was a vital regulator of diploidization, which was consistent with a previous report (Olbrich et al., 2017). However, the exact mechanism by which *p53* triggers diploidization remains unknown. In addition to gene modification, we optimized the TSC culture medium with a serum-free system, named TX medium (Kubaczka et al., 2014). Haploidy was better sustained in TX medium than in traditional TSC (70CM) medium (Tanaka et al., 1998), potentially due to some unknown ingredients in serum (data not shown). In another parallel experiment, we attempted to derive haploid TSCs from haploid blastocysts in TX medium. However, no haploid cell line was established, mainly because embryonic TSCs tended to diploidize more severely. This leaves an open question: can haploid TSCs be established directly from haploid embryos and what is the mechanism underlying the thorough diploidization of haploid TE? We can compare the transcriptome differences between haiTSCs and haploid TEs from blastocysts in a future study.

As our haiTSCs were generated from haESCs *in vitro*, their purity and TSC properties needed to be confirmed. CDCP1 is a TSC-specific marker that has been widely used in research related to trophoblast cell fate determination (Rugg-Gunn et al., 2012; Nosi et al., 2017). Although our haiTSCs were established from an inducible system, a high percentage of CDCP1-positive cells was obtained (Figure 3A) after two rounds of FACS, and these cells maintained TSC properties. haiTSCs were maintained in a haploid state assisted by Hoechst 33342 purification and possessed differentiation potential to mimic placental

development (Figures S5C and 3G), even contributing to functional placenta according to a chimeric experiment (Figures 3H and 3I). These features make haiTSCs perfect tools to evaluate the function of recessive genes related to placental development. Recently, the derivation of human TSCs was reported, raising extensive concerns regarding the study of placental abnormality in diseases associated with abortion (Okae et al., 2018). In this study, haiTSCs served as a platform to screen essential placental development genes through reverse genetic screening. Abundant mutations were introduced into haiTSCs by the PB transposon (Figures 4D, S6A and S6B), consistent with a previous report (Wang et al., 2018). Stable maintenance of haploidy by haiTSCs facilitated the production of homozygous mutant libraries (Figure 4C), which are quite valuable for genetic screening. Therefore, in this study, we used haiTSCs in high-throughput screening to identify *Htra1* as a crucial gene regulating trophoblast specification. Early cell fate determination induces blastomeres to divide into the TE and ICM (Vogel, 2005; Takaoka and Hamada, 2012); however, the molecular mechanism remains unclear. haiTSCs can also serve as a tool for the discovery of key genes regulating TE and ICM interactions.

In summary, we converted haESCs to haiTSCs by controlling the expression level of *Cdx2* with a Dox-inducible system. Although diploidization accompanied the conversion process, deletion of the *p53* gene reduced diploidization to some degree and facilitated the derivation of haiTSCs. haiTSCs not only showed standard TSC colonies and expressed TSC-specific genes but also held the potential to differentiate into placental cells. Therefore these haploid extraembryonic progenitor cells show great advantages for trophoblast lineage genetic screening.

Limitations of the Study

In this experiment, we adapted p53 knockout strategy to establish authentic haploid extraembryonic cell line in a haploid nature. Whether the p53 knockout method could also benefit derivation of haploid TSCs from haploid blastocysts remains unknown. Meanwhile, p53 is an essential gene related to many important biological processes, including mitosis (Cross et al., 1995) and cancer (Li et al., 2010). Strikingly, p53 knockout rescued the viability of tetraploid ESCs and enabled the generation of late-stage mouse tetraploid embryos (Horii et al., 2015). Whether p53 knockout genotype would affect some unknown function of haiTSCs warrants more investigations.

METHODS

All methods can be found in the accompanying Transparent Methods supplemental file.

SUPPLEMENTAL INFORMATION

Supplemental Information includes Transparent Methods, seven figures, and one table and can be found with this article online at https://doi.org/10.1016/j.isci.2018.12.014.

AUTHOR CONTRIBUTIONS

L.S. designed and supervised this project. K.P., X.L., Y.W., J.Z., Q.G., W.Z., and Q.Z. performed the experiments. J.Y. and C.W. analyzed the bioinformatics. L.S.,Y.F., and Y.Y. wrote the manuscript with contribution by all authors.

DECLARATION OF INTERESTS

The authors declare no competing interests.

REFERENCES

Benchetrit, H., Herman, S., van Wietmarschen, N., Wu, T., Makedonski, K., Maoz, N., Yom Tov, N., Stave, D., Lasry, R., and Zayat, V. (2015). Extensive nuclear reprogramming underlies lineage conversion into functional trophoblast stem-like cells. Cell Stem Cell 17, 543–556.

Cross, S.M., Sanchez, C.A., Morgan, C.A., Schimke, M.K., Ramel, S., Idzerda, R.L., Raskind, W.H., and Reid, B.J. (1995). A p53-dependent mouse spindle checkpoint. Science 267, 1353–1356.

Elling, U., Taubenschmid, J., Wirnsberger, G., O'Malley, R., Demers, S.P., Vanhaelen, Q., Shukalyuk, A.I., Schmauss, G., Schramek, D., Schnuetgen, F., and von Melchner, H. (2011). Forward and reverse genetics through derivation of haploid mouse embryonic stem cells. Cell Stem Cell 9, 563–574.

Gao, Q., Zhang, W., Ma, L., Li, X., Wang, H., Li, Y., Freimann, R., Yu, Y., Shuai, L., and Wutz, A. (2018). Derivation of haploid neural stem cell lines by selection for a Pax6-GFP reporter. Stem Cells Dev. 27, 479–487.

He, W., Zhang, X., Zhang, Y., Zheng, W., Xiong, Z., Hu, X., Wang, M., Zhang, L., Zhao, K., Qiao, Z., and Lai, W. (2018). Reduced self-diploidization and improved survival of semi-cloned mice produced from androgenetic haploid embryonic stem cells through overexpression of Dnmt3b. Stem Cell Reports 10, 477–493.

He, Z.Q., Xia, B.L., Wang, Y.K., Li, J., Feng, G.H., Zhang, L.L., Li, Y.H., Wan, H.F., Li, T.D., Xu, K., and Yuan, X.W. (2017). Generation of mouse haploid somatic cells by small molecules for genome-wide genetic screening. Cell Rep. 20, 2227–2237.

Horii, T., Yamamoto, M., Morita, S., Kimura, M., Nagao, Y., and Hatada, I. (2015). p53 suppresses tetraploid development in mice. Sci. Rep. 5, 8907.

Kubaczka, C., Senner, C., Arauzo-Bravo, M.J., Sharma, N., Kuckenberg, P., Becker, A., Zimmer, A., Brustle, O., Peitz, M., Hemberger, M., and Schorle, H. (2014). Derivation and maintenance of murine trophoblast stem cells under defined conditions. Stem Cell Reports 2, 232–242.

Kubaczka, C., Senner, C.E., Cierlitza, M., Arauzo-Bravo, M.J., Kuckenberg, P., Peitz, M., Hemberger, M., and Schorle, H. (2015). Direct induction of trophoblast stem cells from murine fibroblasts. Cell Stem Cell 17, 557–568.

Latos, P.A., and Hemberger, M. (2016). From the stem of the placental tree: trophoblast stem cells and their progeny. Development 143, 3650–3660.

Leeb, M., Dietmann, S., Paramor, M., Niwa, H., and Smith, A. (2014). Genetic exploration of the exit from self-renewal using haploid embryonic stem cells. Cell Stem Cell 14, 385–393.

Leeb, M., and Wutz, A. (2011). Derivation of haploid embryonic stem cells from mouse embryos. Nature 479, 131–134.

Li, M., Fang, X., Baker, D.J., Guo, L., Gao, X., Wei, Z., Han, S., van Deursen, J.M., and Zhang, P. (2010). The ATM-p53 pathway suppresses aneuploidy-induced tumorigenesis. Proc. Natl. Acad. Sci. U S A 107, 14188–14193.

Li, Y., and Shuai, L. (2017). A versatile genetic tool: haploid cells. Stem Cell Res. Ther. 8, 197.

Liu, L., Trimarchi, J.R., and Keefe, D.L. (2002). Haploidy but not parthenogenetic activation leads to increased incidence of apoptosis in mouse embryos. Biol. Reprod. 66, 204–210.

Ng, R.K., Dean, W., Dawson, C., Lucifero, D., Madeja, Z., Reik, W., and Hemberger, M. (2008). Epigenetic restriction of embryonic cell lineage fate by methylation of Elf5. Nat. Cell Biol. 10, 1280–1290.

Niwa, H., Toyooka, Y., Shimosato, D., Strumpf, D., Takahashi, K., Yagi, R., and Rossant, J. (2005). Interaction between Oct3/4 and Cdx2 determines trophectoderm differentiation. Cell 123, 917–929.

Nosi, U., Lanner, F., Huang, T., and Cox, B. (2017). Overexpression of trophoblast stem cell-enriched MicroRNAs promotestrophoblast fate in embryonic stem cells. Cell Rep. 19, 1101–1109.

Oda, M., Shiota, K., and Tanaka, S. (2006). Trophoblast stem cells. Methods Enzymol. 419, 387–400.

Okae, H., Toh, H., Sato, T., Hiura, H., Takahashi, S., Shirane, K., Kabayama, Y., Suyama, M., Sasaki, H., and Arima, T. (2018). Derivation of human trophoblast stem cells. Cell Stem Cell 22, 50–63.e6.

Olbrich, T., Mayor-Ruiz, C., Vega-Sendino, M., Gomez, C., Ortega, S., Ruiz, S., and Fernandez-Capetillo, O. (2017). A p53-dependent response limits the viability of mammalian haploid cells. Proc. Natl. Acad. Sci. U S A 114, 9367–9372.

Rugg-Gunn, P.J., Cox, B.J., Lanner, F., Sharma, P., Ignatchenko, V., McDonald, A.C., Garner, J., Gramolini, A.O., Rossant, J., and Kislinger, T. (2012). Cell-surface proteomics identifies lineage-specific markers of embryo-derived stem cells. Dev. Cell 22, 887–901.

Sagi, I., Chia, G., Golan-Lev, T., Peretz, M., Weissbein, U., Sui, L., Sauer, M.V., Yanuka, O., Egli, D., and Benvenisty, N. (2016). Derivation and differentiation of haploid human embryonic stem cells. Nature 532, 107–111.

Shuai, L., Wang, Y., Dong, M., Wang, X., Sang, L., Wang, M., Wan, H., Luo, G., Gu, T., Yuan, Y., et al. (2015). Durable pluripotency and haploidy in epiblast stem cells derived from haploid embryonic stem cells in vitro. J. Mol. Cell Biol. 7, 326–337.

Shuai, L., and Zhou, Q. (2014). Haploid embryonic stem cells serve as a new tool for mammalian genetic study. Stem Cell Res. Ther. 5, 20.

Strumpf, D., Mao, C.A., Yamanaka, Y., Ralston, A., Chawengsaksophak, K., Beck, F., and Rossant, J. (2005). Cdx2 is required for correct cell fate specification and differentiation of trophectoderm in the mouse blastocyst. Development 132, 2093–2102.

Takahashi, S., Lee, J., Kohda, T., Matsuzawa, A., Kawasumi, M., Kanai-Azuma, M., Kaneko-Ishino, T., and Ishino, F. (2014). Induction of the G2/M transition stabilizes haploid embryonic stem cells. Development 141, 3842–3847.

Takaoka, K., and Hamada, H. (2012). Cell fate decisions and axis determination in the early mouse embryo. Development 139, 3–14.

Tanaka, S., Kunath, T., Hadjantonakis, A.K., Nagy, A., and Rossant, J. (1998). Promotion of trophoblast stem cell proliferation by FGF4. Science 282, 2072–2075.

Vogel, G. (2005). Embryology. Embryologists polarized over early cell fate determination. Science 308, 782–783.

Wang, H., Zhang, W., Yu, J., Wu, C., Gao, Q., Li, X., Li, Y., Zhang, J., Tian, Y., Tan, T., et al. (2018). Genetic screening and multipotency in rhesus monkey haploid neural progenitor cells. Development 145, https://doi.org/10.1242/dev.160531.

Wu, T., Wang, H., He, J., Kang, L., Jiang, Y., Liu, J., Zhang, Y., Kou, Z., Liu, L., Zhang, X., and Gao, S. (2011). Reprogramming of trophoblast stem cells into pluripotent stem cells by Oct4. Stem Cells 29, 755–763.

Ying, Q.L., Wray, J., Nichols, J., Batlle-Morera, L., Doble, B., Woodgett, J., Cohen, P., and Smith, A. (2008). The ground state of embryonic stem cell self-renewal. Nature 453, 519–523.

Supplemental Information

Derivation of Haploid Trophoblast

Stem Cells via Conversion *In Vitro*

Keli Peng, Xu Li, Congyu Wu, Yuna Wang, Jian Yu, Jinxin Zhang, Qian Gao, Wenhao Zhang, Qian Zhang, Yong Fan, Yang Yu, and Ling Shuai
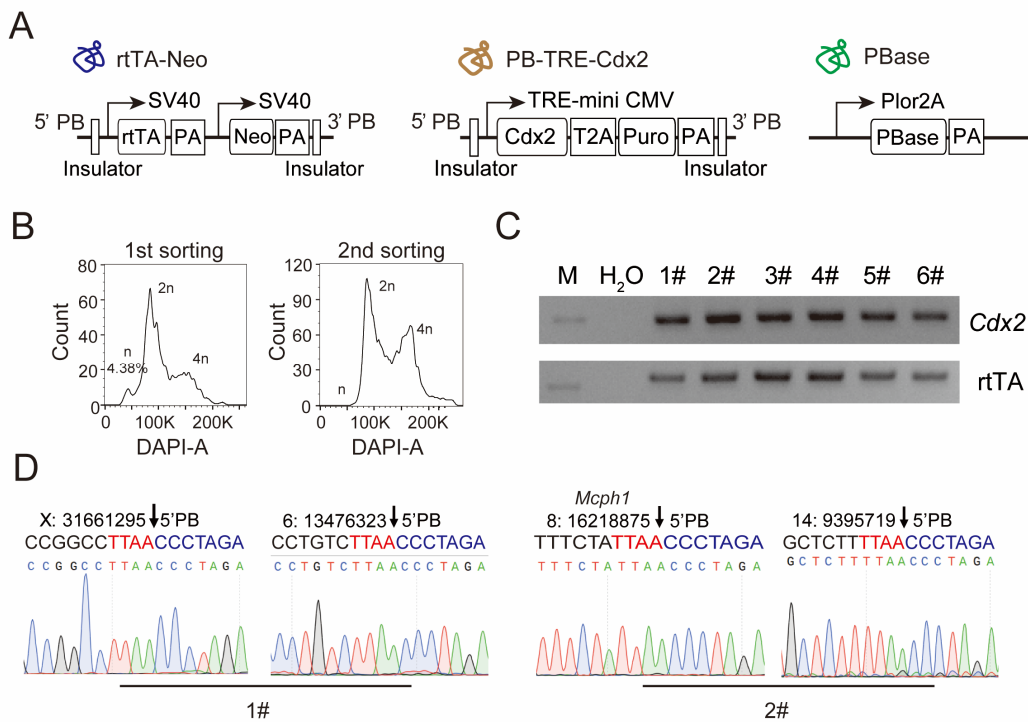
Figure S1 related to Figure 1

(A) Schematic overview of the vectors used for overexpression of *Cdx2*. There are three vectors: vector 1 has the *rtTA* and *Neo* selection genes; vector 2 has the *Cdx2* coding region and *Puromycin* resistance gene driven by TRE with a minimal CMV promoter; vector 3 is used as a PBase expression vector.

(B) DNA content analysis of the cells on Day 11 (first sorting) and Day 23 (second sorting) during conversion.

(C) Genotype of the six subclones from OE-Cdx2 haESCs with *Cdx2* and rtTA indicated.

(D) Sequencing traits of insertion sites of PB in #1 and #2.
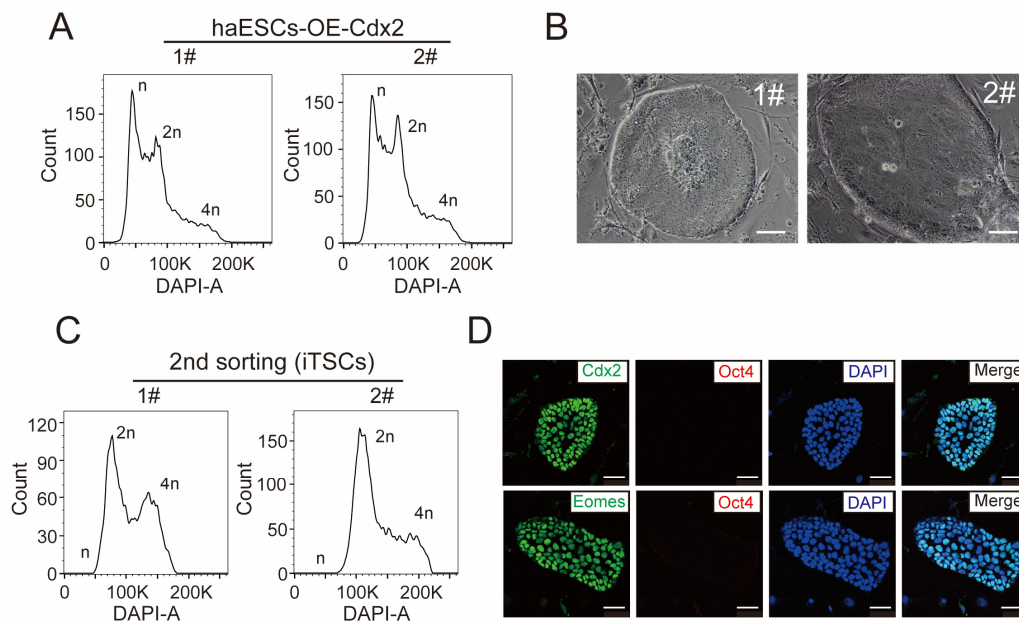
Figure S2 related to Figure 1

(A) DNA content analysis of two stable haploid transgenic OE-Cdx2 cell lines, #1 and #2.

(B) The morphology of iTSCs from subclones #1 and #2. Scale bar, 100 μm.

(C) DNA content analysis of the cells converted from #1 and #2 on Day 23 (second sorting).

(D) Immunofluorescence staining of Oct4 (TRITC channel), Eomes (FITC channel) and Cdx2 (FITC channel) in iTSCs. DNA is stained with DAPI. Scale bar, 50 μm.
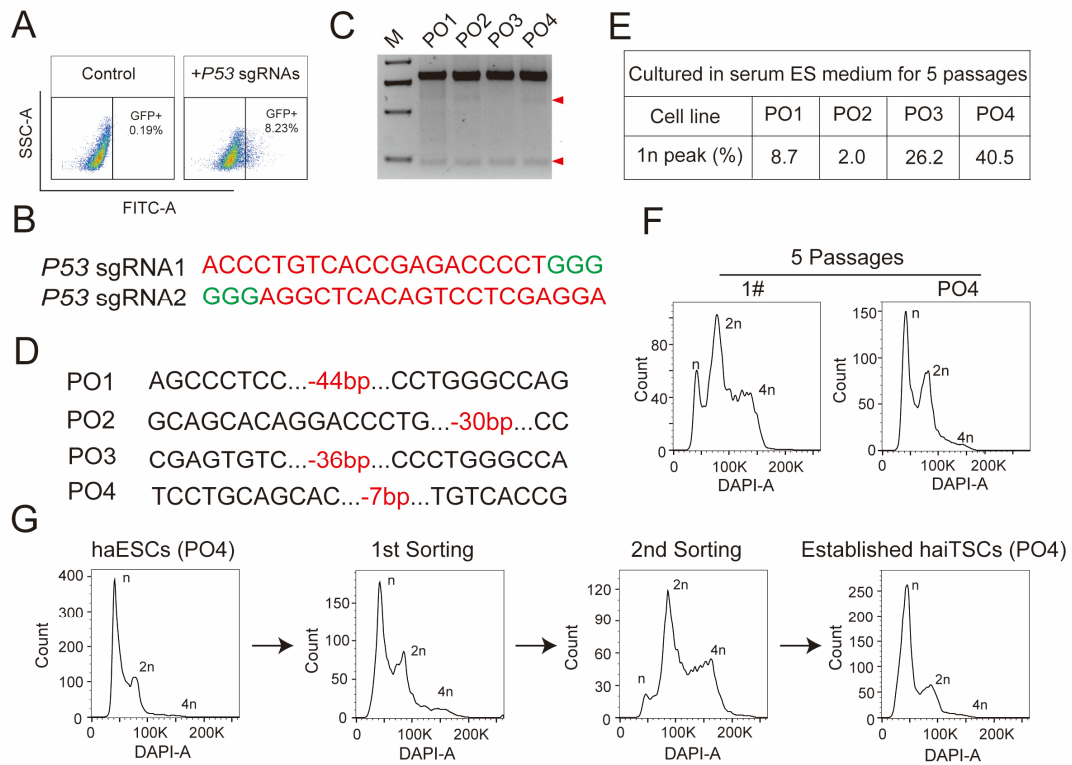
Figure S3 related to Figure 2

(A) Percentage of Cas9-GFP-positive cells in #1 by FACS 2 days after transfection.

(B) sgRNA sequences used for P53 knockout.

(C) *P53*-deleted genotypes in subclones PO1, PO2 and PO3.

(D) Percentages of the 1n peaks of four P53 knockout subclones, PO1, PO2, PO3 and PO4, cultured in serum ES medium for 5 passages.

(E) T7ENI cleavage analysis of the *P53* knockout cell lines PO1, PO2, PO3 and PO4. Cleaved products (red triangle) indicate the presence of mutations.

(F) DNA content analysis of #1 and PO4 cultured in 2i/L medium.

(G) DNA content analysis of cells during conversion on Day 0, Day 11, and Day 23 and final established haiTSCs. The percentages of the 1n (G0/G1) peak were 69.4%, 53.2%, 6.59%, and 70.4%, respectively.
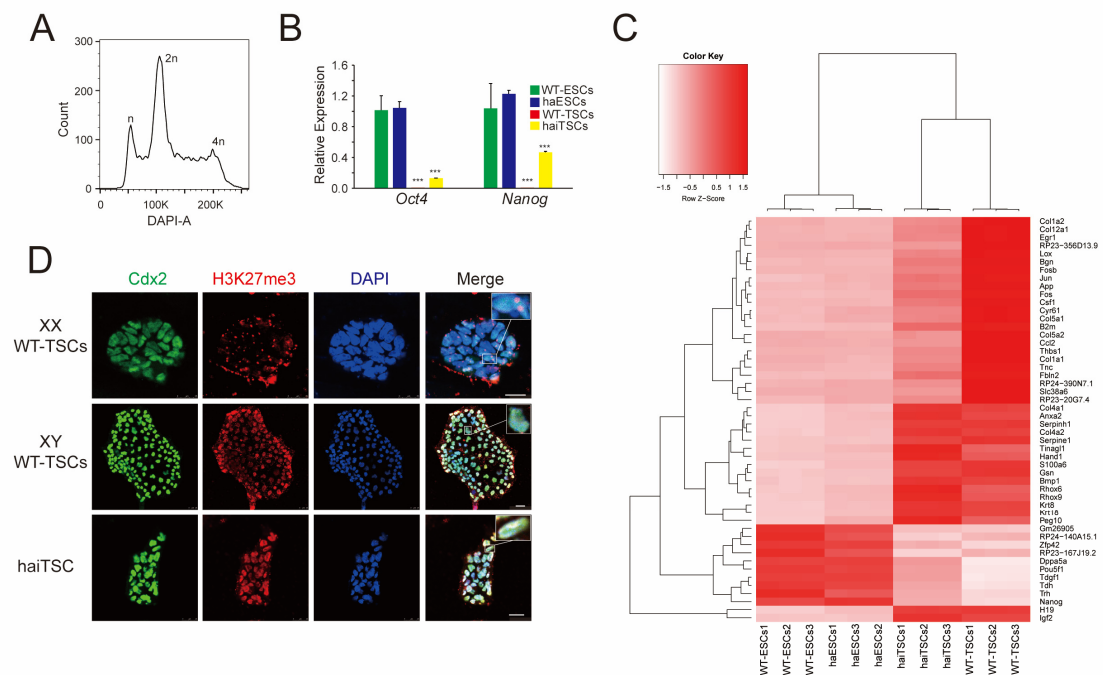
Figure S4 related to Figure 3

(A) DNA content analysis of haiTSCs after CDCP1 antibody sorting and expansion. The percentage of the 1n (G0/G1) peak was 15.3%.

(B) Expression level analysis of pluripotent marker genes (*Oct4* and *Nanog*) in haiTSCs, WT-TSCs, haESCs and WT-ESCs by qPCR. t test, ***$p < 0.001$. Data are represented as mean±SEM.

(C) Heatmap of the top 50 most variable genes across all four cell types. Data are first scaled by row and then represented using hierarchical clustering for both samples and genes.

(D) Immunofluorescence staining of Cdx2 (FITC channel) and H3K27me3 (TRITC channel) in female WT-TSCs, male WT-TSCs and haiTSCs. Female WT-TSCs (XX) and male (XY) WT-TSCs are used as controls. DNA is stained with DAPI. Scale bar, 50 μm.
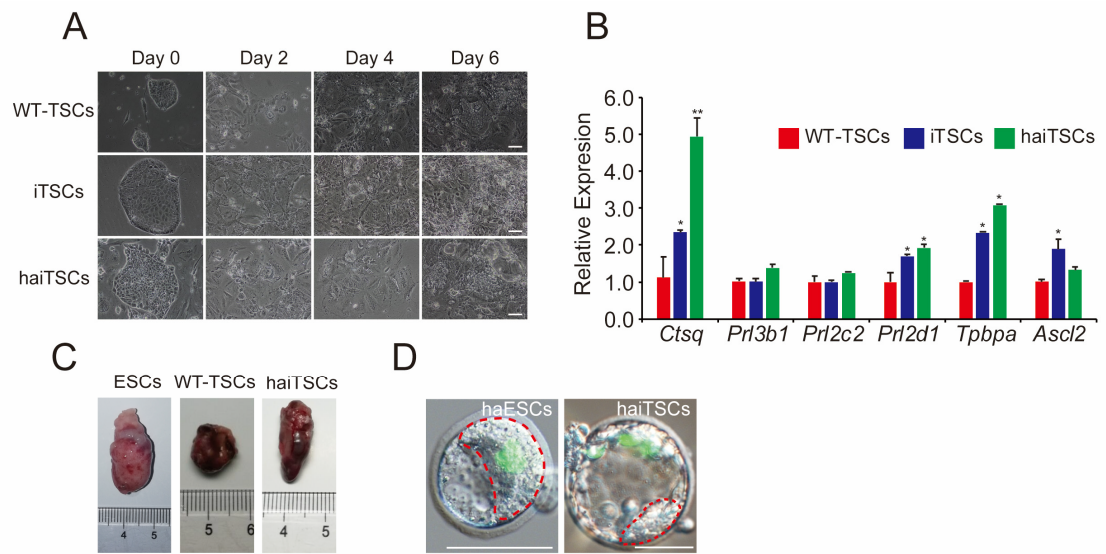
Figure S5 related to Figure 3

(A) Brightfield images of haiTSCs grown in differentiation medium (TS medium without F4H) on Day 0, Day 2, Day 4 and Day 6. Scale bar, 50 μm.

(B) The expression levels of trophoblast lineage-specific gene markers (Ctsq, Prl3b1, Prl2c2, Prl3d1, Tpbpa and Ascl2) in 4-day differentiated cells from WT-TSCs, iTSCs (diploid) and haiTSCs. t test, *p < 0.05, **p < 0.01. Data are represented as mean±SEM.

(C) Teratomas derived from ESCs and hemorrhagic lesions derived from WT-TSCs and haiTSCs.

(D) Reconstructed chimeric blastocysts, with separate contributions of GFP-haESCs (left) and GFP-haiTSCs (right). The red dashed line indicates the area of the inner cell mass. Scale bar, 40 μm.

A

NO.	Insertion Gene	Position	Chromosome	PB orientation
1	NA	Intergenic region	11	NA
2	Ptprd	Intron	4	Reverse
3	NA	Intergenic region	13	NA
4	Bach2	Intron	4	Forward
5	Csf3	Extron	11	Reverse
6	NA	Intergenic region	1	NA
7	Kif1b	Intron	4	Forward
8	Btk	Intron	X	Forward
9	Mllt3	Intron	4	Forward
10	NA	Intergenic region	X	NA
11	Gm27943	Extron	1	Reverse
12	NA	Intergenic region	4	NA
13	P4htm	Intron	17	Forward
14	Glb1l	Extron	1	Reverse
15	NA	Intergenic region	10	NA
16	Runx1	Intron	16	Reverse
17	Mamld1	Intron	X	Forward
18	Fgf14	Intron	1	Reverse
19	NA	Intergenic region	9	NA
20	Zfp236	Intron	18	Forward
21	NA	Intergenic region	8	NA
22	NA	Intergenic region	4	NA
23	NA	Intergenic region	11	NA
24	Btbd11	Intron	10	Forward
25	NA	Intergenic region	11	NA
26	NA	Intergenic region	6	NA
27	Usp7	Intron	16	Reverse
28	Cstf1	Intron	2	Reverse
29	Man1c1	Intron	4	Forward
30	P4htm	Intron	9	Forward
31	NA	Intergenic region	13	NA
32	NA	Intergenic region	4	NA
33	NA	Intergenic region	6	NA
34	NA	Intergenic region	16	NA
35	NA	Intergenic region	2	NA
36	Arntl	Intron	7	Forward
37	Asb6	Intron	2	Forward
38	NA	Intergenic region	10	Forward
39	Slco1a6	Intron	6	Reverse
40	Crtac1	Intron	19	Reverse
41	NA	Intergenic region	6	NA
42	NA	Intergenic region	18	NA
43	NA	Intergenic region	9	NA
44	NA	Intergenic region	5	NA
45	NA	Intergenic region	X	NA
46	Zmynd8	Intron	2	Forward
47	NA	Intergenic region	11	NA
48	Epb41l4a	Intron	2	Forward
49	NA	Intergenic region	1	NA
50	NA	Intergenic region	11	NA

B

Intron 21
Intergenic region 26
Extron 3

C

Control
Trapping
Repeat 2
D3 diff.

D

Repeat 2
Control — Trapping
SSC-A
Tpbpa+ 1.41%
Tpbpa+ 10.6%
FITC-A

Figure S6 related to Figure 4

(A) Detected insertion sites of randomly picked subclones by Splinkerette PCR.

(B) Summary of the detected integrated sites.

(C) Brightfield images of differentiated cells from mutated (trapping) and nonmutated haiTSCs (control) in a single repeat. Scale bar, 100 μm.

(D) FACS analysis of Tpbpa-positive cells in differentiated cells from the trapping and control groups in the same repeat.

Figure S7 related to Figure 5

(A-I) Strand-specific coverage tracks of the genes *Zfp704*, *Rsf1*, *Tead4*, *Tead1*, *Pbx3*, *Esrrb*, *Nfkb1*, *Smad3* and *Tet1* for the selected library (red).

Table S1. Primer Sequences, related to Figures 1, 2, 3, 4 and 6.

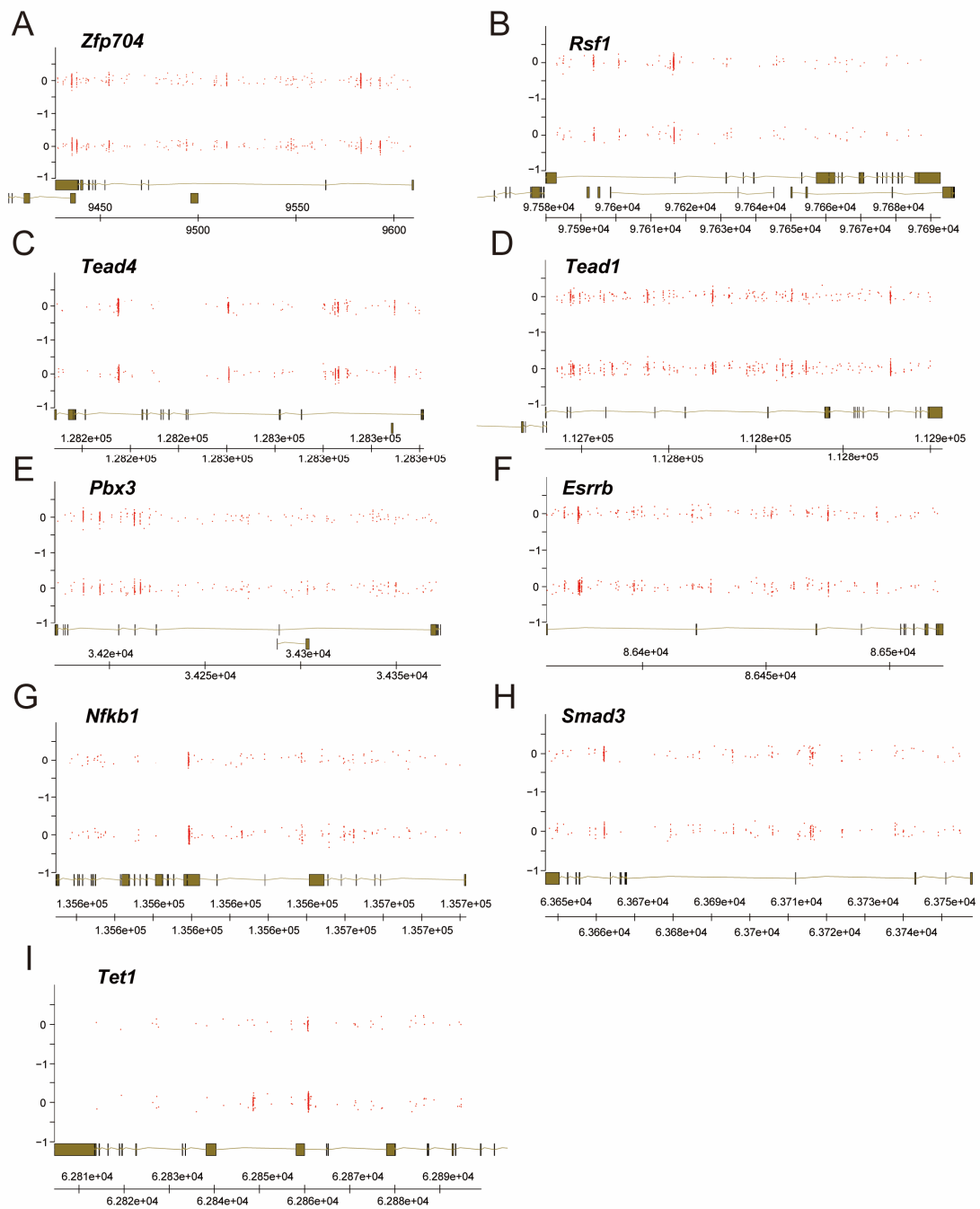| Genotyping	Target Name	Sequence 5'-3'
	AD	F: TATGCCAAGTACGCCCCCTA
	AD	R: AGTAATTCCAGAGCGCCGTT
	OE	F: GGTGACGTGGAGGAGAATCC
	OE	R: CTCGTAGAAGGGGAGGTTGC
	Htra1	F: GGCCAATGGGCTTAACCGT
	Htra1	R: GACTGGTCGGGCTGAGTTG
Construct vector		
	rtTA-neo	F: CCTACTAGTCACGGATCCAGACATGATAAGATACATT
	rtTA-neo	R: TCACACGCGTCACGGTACCTTACTTAGTTACCCGGGG
	Cdx2	F:GAGCTCGGTACCCGGGGATCCATGTACGTGAGCTACCTTCTG
	Cdx2	R: ACGCGTCTGGGTGACAGTGGAGTT
	Puro	F: GTCACCCAGACGCGTGaGGGcaGaGGaaGtcttc
	Puro	R: GCTGCCACTGTTTCTTTAGG
qPCR		
	Gapdh	F: AGGTCGGTGTGAACGGATTTG
	Gapdh	R: TGTAGACCATGTAGTTGAGGTCA
	Oct4	F: GGATGGCATACTGTGGACCTC
	Oct4	R: TTTCATGTCCTGGGACTCCTCG
	Nanog	F: CCAGGGCTATCTGGTGAACG
	Nanog	R: CCCGAAGTTATGGAGCGGAG
	Rex1	F: CCCTCGACAGACTGACCCTAA
	Rex1	R: TCGGGGCTAATCTCACTTTCAT
	Cdx2	F: GTCCCTAGGAAGCCAAGTGAA
	Cdx2	R: TTGGCTCTGCGGTTCTGAAA
	Eomes	F: GGAAGTGACAGAGGACGGTG
	Eomes	R: TTGGCGAAGGGGTTATGGTC
	Elf5	F: TCTGCTGCGACCAGTACAAG
	Elf5	R: GGAGTAACCTTGCGAGCGAA
	Tfap2C	F: ATCCCTCACCTCTCCTCTCC
	Tfap2c	R: CCAGATGCGAGTAATGGTCGG
	Ctsq	F: AGGCTATGTGACTCGTGTGA
	Ctsq	R: GGCACCAGTCACAGGAAAAG
	Prl3b1	F: CCAGAAAACAGCGAGCAAGT
	Prl3b1	R: CCAGGCTTGTAAAATAGTGATGG
	Prl2c2	F: GCCGGCAGTTTGTCTCATAA
	Prl2c2	R: TGAGCCCGAGCACGTTAGAA

	Tpbpa	F: GCTATAGTCCCTGAAGCGCA
	Tpbpa	R: ACTCCACACTGCTTTTATGAGA
	Prl3d1	F: GCCGCAGATGTGTATAGGGA
	Prl3d1	R: AGGGGAAGTGTTCTGTCTGT
	P53	F: CATGAACCGCCGACCTATCC
	P53	R: GCAGTTCAGGGCAAAGGACT
	P21	F: CCCGAGAACGGTGGAACTTT
	P21	R: AGAGTGCAAGACAGCGACAA
	Reprimo	F: TCGCAGTCATGTGTGTGCTC
	Reprimo	R: GCCTCCGGTCCTTCACTAGG
	Cdk1	F: ACACACGAGGTAGTGACGC
	Cdk1	R: TCTGAGTCGCCGTGGAAAAG
	Ascl2	F: AAGCACACCTTGACTGGTACG
	Ascl2	R: AAGTGGACGTTTGCACCTTCA
	Gcm1	F: GCTCCACAGAGGAAGGCCGC
	Gcm1	R: GTTGGTGACCGGGAAGCCGC
Splinkerette PCR		
	Adaptor top	GTTCCCATGGTACTACTCATATAATACGACTCACTATAGG TGACAGCGAGCGCT
	Adaptor bottom	GCGCTCGCTGTCACCTATAGTGAGTCGTATTATAATTTTT TTTCAAAAAAA
	Adaptor	R1: GTTCCCATGGTACTACTCATA
	PB5'	F1: GATATACAGACCGATAAAACACATGCGTCA
	PB3'	F1: GACGGATTCGCGCTATTTAGAAAGAGAG
	Adaptor	R2: TAATACGACTCACTATAGG
	PB5'	F2: ACGCATGATTATCTTTAACGTACGTCAC
	PB3'	F2: CATGCGTCAATTTTACGCAGACTATC
P53 knockout sgRNA		
	sgRNA1-1	CACCGAGGAGCTCCTGACACTCGGA
	sgRNA1-2	AAACTCCGAGTGTCAGGAGCTCCTC
	sgRNA2-1	CACCGACCCTGTCACCGAGACCCCT
	sgRNA2-2	AAACAGGGGTCTCGGTGACAGGGTC
Htra1 knockout sgRNA		
	sgRNA1-1	CACCGGCCGCGTCCGCGACGCGTG
	sgRNA1-2	AAACCACGCGTCGCGGACGCGGCC

Transparent Methods

Animal use and care

Specific pathogen-free (SPF) grade mice were purchased from Beijing Vital River Laboratory Animal Technology Co. Ltd. All animal procedures were performed under the ethical guidelines of Nankai University Animal Center. Female 129Sv/Jae mice were sacrificed to provide oocytes for the establishment of haESCs and haiTSCs.

Cell Culture

HaESCs were cultured as described previously (Li et al., 2012). TSC medium was made according to a previous report (Tanaka et al., 1998) with slight modification. Briefly, we used a combined TSC medium termed 70CM, containing 30% RPMI 1640 (Thermo) and supplemented with 20% FBS (BI), 2 mM L-glutamine (Sigma), 25 ng/ml human recombinant FGF4 (PeproTech) and 1 μg/ml heparin (Millipore), and 70% MEF conditioned medium with the same supplements. To culture WT-TSCs and stable haiTSCs in chemically defined medium, cells were grown on Matrigel (BD)-coated or feeder-coated dishes in TX medium as described previously (Kubaczka et al., 2014). For differentiation experiments, TS medium lacking FGF4 and heparin was used.

Vector construction

For vector 1, the *PiggyBac* Dual Promoter was digested by *BamHI* and *KpnI* (Thermo), and rtTA and Neo were inserted. For vector 2, the *PiggyBac* Dual promoter was digested by *XhoI* and *EcoRV*, and the TRE, Cdx2 coding sequence and Puro fragments were inserted. *P53*-targeting sgRNAs were created with the CRISPR design tool (www.crispr.mit.edu). The pSpCas9 (BB)-2A-GFP (PX458) vector was digested and dephosphorylated by *BbsI* and *FastAP* (Fermentas). Single-strand oligonucleotides were synthesized and phosphorylated by *T4PNK* (Takara Japan), and a pair of oligonucleotides was annealed and ligated into lined PX458 to generate knockout plasmids. All plasmids were purchased from Addgene (USA). All primers used are listed in Table S1.

Transfection

To obtain OE-Cdx2 cell lines, approximately 1×10^6 haESCs were electroporated with 6 μg of vector 1 or vector 2 and 2 μg of transposase vector by using an electroporator (Invitrogen) at 1,400 V, 10 μs with three pulses. For vector 1 selection, cells were treated with 250 μg/ml G418 (Thermo) for 7 days. Neomycin-resistant cells were purified for haploid cells. For deletion of *P53*, approximately 1×10^6 cells were transfected with 4 μg of sgRNA-Cas9 plasmid. Cas9-GFP-positive cells were sorted 36 hours after transfection by flow cytometry. For the gene trapping experiment, a combination of 10 μg of PBase plasmid and 30 μg of *piggyBac* plasmid (designs see Figure 4A) was electroporated into 1×10^7 haiTSCs using the same conditions as described above (Wang et al., 2018). Puromycin-resistant cells were harvested for Splinkerrette PCR.

Generation of induced TSCs from haESCs *in vitro*

OE-Cdx2 haESCs were seeded at a density of 1×10^5 per well of a six-well plate containing feeder cells and cultured in ESC medium for the first 24 hours. To initiate induction, cells were cultured in TSC media with doxycycline (1 μg/ml) and puromycin (1 μg/ml). Puromycin was withdrawn after 5 days of selection. The medium was refreshed every day until Day 11 to enrich haploid cells, as shown by Hoechst 33342 staining. Haploid cells were sorted according to a previous report (Shuai et al., 2014) a second time after another 12 days. Enriched haploid cells were expanded, and FACS was performed with the CDCP1 antibody as

described previously (Rugg-Gunn et al., 2012).

Immunostaining, AP staining, and karyotype Analysis

Before staining, cells were fixed with 4% paraformaldehyde. Permeabilization was performed with 0.3% Triton X-100 (Sigma) for 40 minutes, and then the cells were incubated with 1% BSA (Sigma) for 1 hour at room temperature. Samples were incubated with primary antibodies against Oct4 (Abcam), SSEA1 (Santa Cruz), Cdx2 (Abcam), Nanog (Abcam), Eomes (Abcam) and Tpbpa (Abcam) at 4℃ overnight. After three wash steps, the cells were stained with fluorescently coupled secondary antibodies at room temperature for 1 hour. After another three times wash steps, the nuclei were stained with DAPI (YEASEN) for 10 minutes at room temperature. For immunofluorescence: sections were permeabilized with 0.5% Triton X-100 in PBS and then blocked with 5% BSA for 1 h at RT. Slides were then incubated in primary antibody diluted in blocking solution at 4°C overnight. The following primary antibodies were used: Alpha (Ab13970, Abcam), Proliferin (sc-271891, Santa Cruz), GCM1 (sc-101173, Santa Cruz), and Anti-GFP (Ab104401, Abcam). Subsequently, sections were washed with PBST three times and incubated for 1 h at RT in the dark with secondary fluorescence antibodies. The nuclei were stained with Hoechst 33342 for 10 min at RT. AP staining of OE-Cdx2 haESCs was performed as described previously (Zhao et al., 2009). AP staining was performed according to the manufacturer's instructions for the alkaline phosphatase kit (Beyotime). The results were observed under an inverted microscope or laser-scanning confocal microscope. Karyotype analysis was performed following standard instructions.

Quantitative Real-time PCR

Total RNA was purified from cells using Trizol reagent (Thermo), while cDNA was obtained using a Prime Script™ RT Reagent Kit with gDNA Eraser (Takara). Quantitative PCRs were performed with an ABI QuantStudio™ 6 Flex machine using FS Universal SYBR Green Master (Roche). Relative expression levels were normalized to *Gapdh*. Averages and SD values were from three independent experiments. All the primers used are listed in Table S1.

Western blotting

For western blotting experiments, protein samples were extracted by RIPA lysis solution (Solarbio) from ESCs and TSCs. Lysates were precleared by centrifugation for 5 minutes. Equal amounts of cell lysates were separated by SDS-PAGE and transferred to a polyvinylidene fluoride (PVDF) membrane (GE). The membranes were blocked in 5% nonfat dry milk for 1 hour, washed three times by TBST, and incubated with primary antibodies overnight at 4℃. Then, the membranes were washed and incubated with appropriate secondary antibodies for 1 hour at room temperature. Signals on the membrane were detected by using Western Blotting Detection Reagents (Engreen) and imaged. The primary antibodies used for western blotting included anti-Cdx2 (Abcam), anti-Eomes (Abcam) and anti-Gapdh (Abcam).

Bisulphite Sequencing

Genomic DNA of each sample was modified with the EpiTect Bisulfite Kit (Qiagen). Two-round nested PCR was performed to amplify the promoter region of each gene and PCR products were purified from agarose gel by Gel Extraction Kit (OMEGA).Primer sequences were as previous described for Oct4 (Blelloch et al., 2006), Nanog(Takahashi and Yamanaka, 2006) and Elf5(Ng et al., 2008).

Splinkerrette PCR

Splinkerrette PCR was used to find the insertion sites after *piggyBac* transposon transfection as previously described (Uren et al., 2009). Briefly, the genomic DNA purified from cells was digested by *Bsp143I*

(Thermo), and an adenine was added to the tails of fragments by *Taq* DNA Polymerase (Thermo). Purified products were linked to Splinkerrette adaptors for nest PCR. Nest PCR products were linked into pEASY Blunt simple vectors (Transgene) for Sanger sequencing. All primers and Splinkerrette adaptors used are listed in Table S1.

T7ENI assay

Following the manufacturer's recommended protocol (NEB), target DNA fragments containing sgRNA target sites were amplified from transfected cells and wild-type cell genomic DNA by Q5® Hot Start High-Fidelity DNA Polymerase (NEB). The two kinds of fragments were mixed together and annealed in Buffer 2.0 (NEB). T7 Endonuclease I was added into the mixture, and digestion was carried out for 1 hour at 37℃. The products were run on a 2% TAE gel (Biowest), stained with SYBR® Safe DNA gel stain (Thermo) and imaged on a gel imager (Bio-Rad).

TSC Transplantation and immunohistochemistry staining

TSC transplantations were performed as published (Kubaczka et al., 2014). Briefly, $1×10^6$ haiTSCs were resuspended in 200 μl of 70CM containing FGF4/heparin and injected into the testis of 8-week-old male ICR mice. Approximately 21 days postinjection, hemorrhagic lesions were dissected from the testis, fixed in 4% paraformaldehyde overnight, embedded in paraffin, and sectioned. Sections were rehydrated and treated for antigen retrieval in sodium citrate buffer at a sub-boiling temperature. Next, endogenous peroxidase activity was quenched with 3% hydrogen peroxidase at room temperature (RT). For immunohistochemistry: sections were blocked with 5% BSA for 1 hour at RT. The following primary antibodies were used: Tfap2c (sc-12762; Santa Cruz) and CD31 (MA5-13188, Thermo Fisher). For immunofluorescence: sections were permeabilized with 0.5% Triton X-100 in PBS and then blocked with 5% BSA for 1 h at RT. All primary antibodies against Alpha (Ab13970, Abcam), Proliferin (sc-271891, Santa Cruz), GCM1 (sc-101173, Santa Cruz), and Anti-GFP (Ab104401, Abcam) were incubated with samples overnight at 4℃.

Before staining, cells were fixed with 4% paraformaldehyde. Permeabilization was performed with 0.3% Triton X-100 (Sigma) for 40 minutes and then incubated with 1% BSA (Sigma) for 1 hour at RT. Samples were incubated with primary antibodies against Oct4 (Abcam), SSEA1 (Santa Cruz), Cdx2 (Abcam), Nanog (Abcam), Eomes (Abcam) and Tpbpa (Abcam) at 4℃ overnight. After three times washing steps, the samples were stained with fluorescently coupled secondary antibodies at room temperature for 1 hour.

Diploid chimeric assay

Chimeric embryos were generated by injecting haiTSC-GFP cells into CD-1 mouse recipient 4-cell embryos according to a previous protocol (Li et al., 2012), using ES-GFP cells as a control treatment. Diploid 4-cell embryos were collected from the uterus of a 2.5 dpc female CD-1 mouse. Approximately 10-15 ES-GFP cells and FACS-purified G0/G1 phase haiTS-GFP cells were injected into each blastocyst. Then, chimeric embryos were cultured to the blastocyst stage in KSOM (Millipore) for subsequent analysis.

Genetic screening in haiTSCs

HaiTSCs were mutated with trapping vectors (Figure 4A) and treated with puromycin (1 μg/ml) for 1 day. Puromycin-resistant haiTSCs and nontransfected haiTSCs were differentiated in standard TS medium without heparin and FGF4 for 3 days. Cells positive for Tpbpa (Abcam, ab104401) among the differentiated cells were harvested by antibody staining and sorting according to the manufacturer's

instructions. In each repeat, we selected Tpbpa-positive cells in the significantly increasing group relative to the nontransfected group to perform high-throughput sequencing.

Analysis of RNA-seq data

Raw data were trimmed using customized scripts to remove low-quality bases (quality score < 5) or reads (low-quality bases > 50% of the read size). Then, the abundance of each transcript was counted using Kallisto (Bray et al., 2016) with Gencode M18 (Harrow et al., 2006) and further summarized for each gene using the R package tximport (Soneson et al., 2015). Genes covered by less than 2 reads across all samples or with more than 2 samples possessing zero reads were filtered out. Genes were normalized using relative-log-expression (RLE) from DESeq2 (Love et al., 2014). Correlations among samples were measured based on the top 50 most variable genes using cosine distance. To generate the MDS plot of all samples, data were first transformed using the function variance Stabilizing() and then the function plotPCA() from DESeq2 (Love et al., 2014). Plots were visualized by ggplot2 (Ginestet, 2011).

Analysis of *piggyBac* screening data

Reads were mapped to the genome assembly from UCSC (mm10) (Zimin et al., 2014) using bowtie2 (v2.2.3) (Langmead and Salzberg, 2012) under sensitive-local mode. Read distributions across different regions were summarized using RSeQC (v2.6.1) (Wang et al., 2012). VISITs (v0.22) (Yu and Ciaudo, 2017) was used to estimate the number of insertions for each gene using the annotation from Gencode (Harrow et al., 2006), excluding duplicated and multiple-hit reads.

Data were first filtered by removing genes covered by < 2 reads, then normalized using relative-log-expression (RLE) from DESeq2 (v1.10.1) (Love et al., 2014). Log2-transformed fold changes were further calculated based on normalized data. The coverage tracks were generated using R package GenomeGraphs (v1.30) (Bullard, 2016). For enrichment analysis, gene sets were retrieved from the Gene Ontology (Ashburner et al., 2000) and KEGG databases (Kanehisa and Goto, 2000). The top 200 genes with the most abundant insertions were used. Fisher's exact test followed by the Benjamini-Hochberg correction (Benjamini and Hochberg, 1995) was used to generate the FDR.

Supplemental Reference

ASHBURNER, M., BALL, C. A., BLAKE, J. A., BOTSTEIN, D., BUTLER, H., CHERRY, J. M., DAVIS, A. P., DOLINSKI, K., DWIGHT, S. S., EPPIG, J. T., HARRIS, M. A., HILL, D. P., ISSEL-TARVER, L., KASARSKIS, A., LEWIS, S., MATESE, J. C., RICHARDSON, J. E., RINGWALD, M., RUBIN, G. M. & SHERLOCK, G. 2000. Gene ontology: tool for the unification of biology. The Gene Ontology Consortium. *Nat Genet,* 25**,** 25-9.

BENJAMINI, Y. & HOCHBERG, Y. 1995. Controlling the False Discovery Rate - a Practical and Powerful Approach to Multiple Testing. *Journal of the Royal Statistical Society Series B-Methodological,* 57**,** 289-300.

BLELLOCH, R., WANG, Z., MEISSNER, A., POLLARD, S., SMITH, A. & JAENISCH, R. 2006. Reprogramming efficiency following somatic cell nuclear transfer is influenced by the differentiation and methylation state of the donor nucleus. *Stem Cells,* 24**,** 2007-13.

BRAY, N. L., PIMENTEL, H., MELSTED, P. & PACHTER, L. 2016. Near-optimal probabilistic RNA-seq quantification. *Nat Biotechnol,* 34**,** 525-7.

BULLARD, S. D. A. J. 2016. GenomeGraphs: Plotting genomic information from Ensembl. R package version 1.32.0. *Bioconductor*.

GINESTET, C. 2011. ggplot2: elegant graphics for data analysis. *Journal of the Royal Statistical Society: Series A (Statistics in Society)*.

HARROW, J., DENOEUD, F., FRANKISH, A., REYMOND, A., CHEN, C. K., CHRAST, J., LAGARDE, J., GILBERT, J. G., STOREY, R., SWARBRECK, D., ROSSIER, C., UCLA, C., HUBBARD, T., ANTONARAKIS, S. E. & GUIGO, R. 2006. GENCODE: producing a reference annotation for ENCODE. *Genome Biol,* 7 Suppl 1**,** S4 1-9.

KANEHISA, M. & GOTO, S. 2000. KEGG: kyoto encyclopedia of genes and genomes. *Nucleic Acids Res,* 28**,** 27-30.

KUBACZKA, C., SENNER, C., ARAUZO-BRAVO, M. J., SHARMA, N., KUCKENBERG, P., BECKER, A., ZIMMER, A., BRUSTLE, O., PEITZ, M., HEMBERGER, M. & SCHORLE, H. 2014. Derivation and maintenance of murine trophoblast stem cells under defined conditions. *Stem Cell Reports,* 2**,** 232-42.

LANGMEAD, B. & SALZBERG, S. L. 2012. Fast gapped-read alignment with Bowtie 2. *Nat Methods,* 9**,** 357-9.

LI, W., SHUAI, L., WAN, H., DONG, M., WANG, M., SANG, L., FENG, C., LUO, G. Z., LI, T., LI, X., WANG, L., ZHENG, Q. Y., SHENG, C., WU, H. J., LIU, Z., LIU, L., WANG, L., WANG, X. J., ZHAO, X. Y. & ZHOU, Q. 2012. Androgenetic haploid embryonic stem cells produce live transgenic mice. *Nature,* 490**,** 407-11.

LOVE, M. I., HUBER, W. & ANDERS, S. 2014. Moderated estimation of fold change and dispersion for RNA-seq data with DESeq2. *Genome Biol,* 15**,** 550.

NG, R. K., DEAN, W., DAWSON, C., LUCIFERO, D., MADEJA, Z., REIK, W. & HEMBERGER, M. 2008. Epigenetic restriction of embryonic cell lineage fate by methylation of Elf5. *Nat Cell Biol,* 10**,** 1280-90.

RUGG-GUNN, P. J., COX, B. J., LANNER, F., SHARMA, P., IGNATCHENKO, V., MCDONALD, A. C., GARNER, J., GRAMOLINI, A. O., ROSSANT, J. & KISLINGER, T. 2012. Cell-surface proteomics identifies lineage-specific markers of embryo-derived stem cells. *Dev Cell,* 22**,** 887-901.

SHUAI, L., LI, W., WAN, H., ZHAO, X. Y., WANG, L. & ZHOU, Q. 2014. Generation of Mammalian offspring by haploid embryonic stem cells microinjection. *Curr Protoc Stem Cell Biol,* 31**,** 1A 6 1-15.

SONESON, C., LOVE, M. I. & ROBINSON, M. D. 2015. Differential analyses for RNA-seq: transcript-level estimates improve gene-level inferences. *F1000Res,* 4**,** 1521.

TAKAHASHI, K. & YAMANAKA, S. 2006. Induction of pluripotent stem cells from mouse embryonic and adult fibroblast cultures by defined factors. *Cell,* 126**,** 663-76.

TANAKA, S., KUNATH, T., HADJANTONAKIS, A. K., NAGY, A. & ROSSANT, J. 1998. Promotion of trophoblast stem cell proliferation by FGF4. *Science,* 282**,** 2072-5.

UREN, A. G., MIKKERS, H., KOOL, J., VAN DER WEYDEN, L., LUND, A. H., WILSON, C. H., RANCE, R., JONKERS, J., VAN LOHUIZEN, M., BERNS, A. & ADAMS, D. J. 2009. A high-throughput splinkerette-PCR method for the isolation and sequencing of retroviral insertion sites. *Nat Protoc,* 4**,** 789-98.

WANG, H., ZHANG, W., YU, J., WU, C., GAO, Q., LI, X., LI, Y., ZHANG, J., TIAN, Y., TAN, T., JI, W., LI, L., YU, Y. & SHUAI, L. 2018. Genetic screening and multipotency in rhesus monkey haploid neural progenitor cells. *Development,* 145.

WANG, L., WANG, S. & LI, W. 2012. RSeQC: quality control of RNA-seq experiments. *Bioinformatics,* 28**,** 2184-5.

YU, J. & CIAUDO, C. 2017. Vector Integration Sites Identification for Gene-Trap Screening in Mammalian Haploid Cells. *Scientific reports,* 7**,** 44736.

ZHAO, X. Y., LI, W., LV, Z., LIU, L., TONG, M., HAI, T., HAO, J., GUO, C. L., MA, Q. W., WANG, L., ZENG, F. Y. & ZHOU, Q. 2009. iPS cells produce viable mice through tetraploid complementation. *Nature,* 461**,** 86-U88.

ZIMIN, A. V., CORNISH, A. S., MAUDHOO, M. D., GIBBS, R. M., ZHANG, X., PANDEY, S., MEEHAN, D. T., WIPFLER, K., BOSINGER, S. E., JOHNSON, Z. P., THARP, G. K., MARCAIS, G., ROBERTS, M., FERGUSON, B., FOX, H. S., TREANGEN, T., SALZBERG, S. L., YORKE, J. A. & NORGREN, R. B., JR. 2014. A new rhesus macaque assembly and annotation for next-generation sequencing analyses. *Biol Direct,* 9**,** 20.